HHS Public Access

Author manuscript

Nat Microbiol. Author manuscript; available in PMC 2020 April 14.

Published in final edited form as:

Nat Microbiol. 2019 December ; 4(12): 2128–2135. doi:10.1038/s41564-019-0578-3.

Type I interferon-driven susceptibility to *Mycobacterium tuberculosis* is mediated by interleukin-1 receptor antagonist IL-1Ra

Daisy X. Ji[1], **Livia H. Yamashiro**[1], **Katherine J. Chen**[1], **Naofumi Mukaida**[2], **Igor Kramnik**[3], **K. Heran Darwin**[4], **Russell E. Vance**[1,5,6,*]

[1]Division of Immunology and Pathogenesis, Department of Molecular and Cell Biology, University of California, Berkeley, CA 94720 USA

[2]Division of Molecular Bioregulation, Cancer Research Institute, Kanazawa University, Kakuma-machi, Kanazawa 920-1192, Japan

[3]The National Emerging Infectious Diseases Laboratory, Department of Medicine (Pulmonary Center), and Department of Microbiology, Boston University School of Medicine, Boston, MA 02118 USA

[4]Department of Microbiology, New York University School of Medicine, New York, New York, 10016 USA

[5]Cancer Research Laboratory, University of California, Berkeley, CA 94720 USA

[6]Howard Hughes Medical Institute, University of California, Berkeley, CA 94720 USA

Summary

The bacterium *Mycobacterium tuberculosis* (*Mtb*) causes tuberculosis (TB) and is responsible for more human mortality than any other single pathogen[1]. Progression to active disease occurs in only a fraction of infected individuals and is predicted by an elevated type I interferon (IFN) response[2-7]. Whether or how IFNs mediate susceptibility to *Mtb* has been difficult to study due to a lack of suitable mouse models[6-11]. Here we examined B6.*Sst1*^{S} congenic mice that carry the "sensitive" allele of the *Sst1* locus that confers susceptibility to *Mtb*[12-14]. We found that enhanced production of type I IFNs was responsible for the susceptibility of B6.*Sst1*^{S} mice to *Mtb*. Type I IFNs affect the expression of hundreds of genes, several of which have previously been implicated in susceptibility to bacterial infections[6,7,15-18]. Nevertheless, we found that heterozygous deficiency in just a single IFN target gene, *Il1rn*, which encodes IL-1 receptor antagonist (IL-1Ra), is sufficient to reverse IFN-driven susceptibility to *Mtb* in B6.*Sst1*^{S} mice. In addition, antibody-

*Corresponding author. rvance@berkeley.edu.

Author contributions. R.E.V., K.H.D., and D.X.J. designed the experiments. L.H.Y assisted with experiments shown in Figure 4 and Extended Data 5. K.J.C. assisted with experiments shown in Extended Data 3. D.X.J. performed all other experiments. R.E.V. and D.X.J. analyzed the data. I.K. generated the B6.*Sst1*^{S} mice. N.M. generated the anti-IL1-Ra antibody. K.H.D. and I.K. gave technical support and conceptual advice. R.E.V. and D.X.J. prepared the manuscript. All correspondences and requests for materials should be addressed to R.E.V.

Competing interests. The authors declare no competing interests.

mediated neutralization of IL-1Ra provided therapeutic benefit to *Mtb*-infected B6.*Sst1*^{S} mice. Our results illustrate the value of the B6.*Sst1*^{S} mouse to model interferon-driven susceptibility to *Mtb*, and demonstrate that IL-1Ra is an important mediator of type I IFN-driven susceptibility to *Mtb* infections *in vivo*.

Mtb infections in humans result in highly diverse outcomes ranging from asymptomatic lung granulomas to lethal disseminated disease. Active TB is characterized by the uncontrolled replication of bacteria and pathological inflammation in the lungs and other organs. There is no vaccine that reliably protects against pulmonary TB, and although antibiotics can be curative, the long (≥6-month) course of treatment and increasing prevalence of multi-drug resistant *Mtb* strains has spurred a search for alternative therapeutics[19,20]. Recent studies have demonstrated that an enhanced type I interferon (IFN) signature correlates with[4,5] and can predict progression to active TB up to 18 months prior to diagnosis[2,3,6,7]. In addition, a partial loss-of-function polymorphism in the type I IFN receptor (IFNAR1) is associated with resistance to TB in humans[21]. A small number of cases also link IFN treatment during chronic viral infections with increased susceptibility to TB[6,7,22-24]. In addition, numerous animal studies have demonstrated causal roles for type I IFNs in susceptibility to *Mtb*[6,7,9,15,16,25-27] and other bacterial infections[18,28].

Given the potential association between type I IFNs and susceptibility to human TB, we sought to determine the mechanisms by which type I IFNs mediate susceptibility to active TB, with the hope this knowledge could be exploited to develop interventions. Mechanistic studies and initial trials of possible therapeutics require a robust animal model. However, the most commonly used animal model, the C57BL/6 (B6) mouse, does not robustly recapitulate the IFN-driven TB susceptibility that appears to occur in humans. B6.*Ifnar*$^{-/-}$ mice show mild resistance to *Mtb* in the spleen and variable but modest effects in the lungs[8-11,15]. Another model of IFN-driven susceptibility involves treatment of *Mtb*-infected B6 mice with poly-IC, a potent inducer of type I IFNs[9,16]. Such treatment dramatically increases susceptibility to *Mtb* in an *Ifnar*-dependent manner[9,16], but because the IFN is induced artificially via signaling pathways such as TLR3 or MDA5 that may not be engaged by *Mtb* itself, it is unclear if poly-IC treatment mimics the course of IFN-driven disease in humans. The 129 mouse strain shows clear IFN-driven susceptibility to *Mtb*[26], but there are limited tools on this genetic background.

As an alternative approach, we turned to a previously described congenic mouse strain, B6.*Sst1*^{S}, that carries the 10.7Mb ‘super susceptibility to tuberculosis 1’ region of mouse chromosome 1 from C3HeB/FeJ mice on an otherwise B6 genetic background[12,13]. B6.*Sst1*^{S} mice exhibit marked susceptibility to aerosol *Mtb* infection[12,13], though how the *Sst1*^{S} locus confers susceptibility remains incompletely understood. Recent work has established that bone-marrow macrophages (BMMs) from B6.*Sst1*^{S} mice exhibit an enhanced type I IFN response[29,30], as we confirm (Extended Data 1). In addition, we found that infected B6.*Sst1*^{S} lungs exhibited higher levels of *Ifnb* transcripts as compared to B6 (Fig. 1a). To investigate whether this enhanced type I IFN signaling causes the susceptibility of B6.*Sst1*^{S} mice to *Mtb*, we treated *Mtb*-infected mice with an IFNAR1-blocking antibody[31] to inhibit type I IFN signaling. B6.*Sst1*^{S} mice treated with the IFNAR1-blocking

antibody showed significantly decreased bacterial burdens compared to those that only received an isotype control antibody (Fig. 1b). To provide genetic confirmation of this result, we crossed B6.*Sst1*^{S} mice to B6.*Ifnar*$^{-/-}$ mice. *Ifnar* deficiency largely reversed the enhanced susceptibility of B6.*Sst1*^{S} mice to *Mtb* infection. At 25 days post-infection, the lung bacterial burdens of B6.*Sst1*^{S}*Ifnar*$^{-/-}$ mice were significantly lower than those of B6.*Sst1*^{S} mice, and were similar to B6 mice (Fig. 1c). Infected B6.*Sst1*^{S}*Ifnar*$^{-/-}$ mice also survived significantly longer than B6.*Sst1*^{S} mice (Fig. 1d), though there are also clearly *Ifnar*-independent effects of the *Sst1*^{S} locus that act at later time points. By contrast, and consistent with prior reports[8,10,11], *Ifnar* deficiency had little or no effect on *Mtb* disease in wild-type B6 mice. Recent data have suggested that the host protein STING is required for interferon induction to *Mtb*[32-37]. However, crossing B6.*Sst1*^{S} mice to STING-deficient *Sting*$^{gt/gt}$ mice did not significantly reduce bacterial burdens at day-25 compared to B6.*Sst1*^{S} mice (Extended Data 2a). The B6.*Sst1*^{S}*Sting*$^{gt/gt}$ mice did show a slight improvement in survival not seen in the B6 genetic background[36] (Extended Data 2b). Overall our data demonstrate that the *Sst1*^{S} locus acts directly or indirectly to increase type I IFN signaling *in vivo* and thereby exacerbate *Mtb* infection, particularly during the early phases of infection.

Type I IFN negatively regulates anti-bacterial immune responses via multiple mechanisms[6,7,18], including through increased IL-10 levels[15-17], decreased IFNγ signaling[38,39], induction of cholesterol 25-hydroxylase (*Ch25h*)[40], and/or decreased IL-1 levels[15,16,41]. We did not observe significant differences between B6 or B6.*Sst1*^{S} mice in IL-10 or IFNγ levels in the lung during *Mtb* infection (Extended Data 3a, b). Crossing B6.*Sst1*^{S} mice to B6.*Ch25h*$^{-/-}$ mice did not alter day-25 lung bacterial burdens (Extended Data 3c). Moreover, despite clear evidence that type I IFN and IL-1 counter-regulate each other[15,16,41,42], the *Sst1*^{S} locus did not appear to decrease the levels of IL-1 *in vivo*; in fact, we unexpectedly observed higher levels of both IL-1α and IL-1β in the lungs of B6.*Sst1*^{S} mice at 25 days post-infection as compared to B6 mice (Fig. 2a,b, associated CFU in Extended Data 3d). Other inflammatory mediators, including TNF and CXCL1 were similarly elevated in the B6.*Sst1*^{S} mice (Extended Data 3e, f) as was the frequency of CD11b$^+$Ly6G$^+$ cells (neutrophils) in the lungs (Extended Data 3g). The elevated inflammation in B6.*Sst1*^{S} mice was a direct or indirect consequence of elevated type I IFNs, as inflammatory cytokines and neutrophils were reduced in B6.*Sst1*^{S}*Ifnar*$^{-/-}$ mice (Fig. 2a,b and Extended Data 3a,b,e-g).

We reasoned that the high levels of IL-1α/β in B6.*Sst1*^{S} mice may be a consequence of the higher bacterial burdens in these mice, or alternatively, may be causing increased bacterial replication via induction of a pro-bacterial inflammatory milieu, as previously proposed[43,44]. To distinguish these possibilities, we inhibited IL-1 signaling *in vivo* using an anti-IL-1R1 blocking antibody[45] (Fig. 2c, Extended Data 4a). Both B6 and B6.*Sst1*^{S} mice treated with IL-1R1 blocking antibody exhibited increased bacterial burdens compared to mice treated with an isotype control antibody. These results confirm prior evidence that IL-1 is protective in B6 mice[46-52], and extend this observation to B6.*Sst1*^{S} mice as well. Thus, elevated IL-1 levels do not explain the exacerbated infections of B6.*Sst1*^{S} mice. Instead, it appears that elevated IL-1 levels are a consequence of increased bacterial burdens in these mice. Although IL-1 is clearly protective during *Mtb* infection of B6 mice, the elevated levels of IL-1α/β proteins seen in B6.*Sst1*^{S} mice for some reason fail to control *Mtb*.

Type I IFNs induce the expression of hundreds of target genes. However, given that IL-1 signaling is essential for resistance to *Mtb*[46-52], we were particularly interested in *Il1rn*, which encodes the secreted IL-1 receptor antagonist (IL-1Ra)[53]. IL-1Ra binds to IL-1R1 without signaling and blocks binding of IL-1α/β[54] (Fig. 3a). *Il1rn* is induced during *Mtb* infection[15,16] and by type I IFN signaling[55,56]. As expected, B6.*Sst1*^{S} BMMs strongly upregulated *Il1rn* in an *Ifnar*-dependent manner when stimulated with TNF (Fig. 3b). Similarly, *Mtb*-infected B6.*Sst1*^{S} mice had higher levels of IL-1Ra protein in their lungs, as compared to B6 or B6.*Sst1*^{S}*Ifnar*$^{-/-}$ mice (Fig. 3c, Extended Data 4b). These results raised the possibility that the high IL-1 protein levels in B6.*Sst1*^{S} mice are inadequate to protect against infection because of a block in IL-1 signaling.

To assess the levels of functional IL-1 signaling in the lungs of infected mice, we employed an IL-1 reporter bioassay to measure IL-1 activity in cell-free supernatant of dissociated lungs. Despite higher levels of IL-1 proteins, lungs from infected B6.*Sst1*^{S} mice appeared to have generally less functional IL-1 signaling capacity as compared with B6 mice (Fig. 3d, Extended Data 4c). The lower levels of IL-1 signaling seen in B6.*Sst1*^{S} mice was reversed in B6.*Sst1*^{S}*Ifnar*$^{-/-}$ mice (Fig. 3d). The reporter appeared to be a reliable indicator of functional IL-1, as responses in the bioassay were blocked by anti-IL-1R1 antibody (Extended Data 4c). These results underline the importance of measuring IL-1 activity versus merely assessing the levels of IL-1 proteins. However, we noted significant variability in the measurable IL-1 activity in the lungs of *Mtb*-infected mice. In fact, the lungs of some B6.*Sst1*^{S} mice exhibited elevated, rather than reduced, IL-1 activity (e.g., 3 of 17 mice shown in Fig. 3d). In addition, in infections with higher initial doses, we failed to detect a difference in the IL-1 activity in the lungs of B6.*Sst1*^{S} versus B6 mice (an example is shown in Extended Data 4d). Conversely, the susceptibility of B6.*Sst1*^{S} mice is highly consistent (Figs. 1c, 2c, Extended Data 2a, 3c-d, 4a). Thus, we hypothesized that low IL-1 signaling may only be a transient phenotype in B6.*Sst1*^{S} mice. To address this possibility, we assessed the timing of IL-1 activity in the lung by performing a time course experiment (Extended Data 4e). We found that at 14 days post-infection, IL-1 activity measurable by bioassay was low in all strains. At 25 days post-infection, there was marked variability in the measurable IL-1 responses of B6.*Sst1*^{S} mice: some mice exhibited the expected defect in IL-1 activity as compared to B6 or B6.*Sst1*^{S}*Ifnar*$^{-/-}$ mice, whereas others were already exhibiting high IL-1 activity levels. By 36 days post-infection, all mice exhibited high IL-1 activity regardless of genotype. Thus, it appears that once the susceptible phenotype of B6.*Sst1*^{S} mice manifests, and CFU levels rise, the level of functional IL-1 increases concordantly. Interestingly, this late rise in IL-1 activity appears insufficient to protect the mice. It was previously reported that IL-1 acts at early timepoints after infection, i.e., prior to day15 post-infection[57]. At early timepoints, when IL-1 may be acting locally at infection foci, the bioassay (performed on total lung) is unable to detect functional IL-1. Thus, we conclude that although specific infection conditions and assay timepoints can reveal a functional deficit in IL-1 signaling in B6.*Sst1*^{S} mice, our IL-1 bioassay is generally an insensitive tool for measuring protective IL-1 activity *in vivo*.

Given the above considerations, we sought genetic evidence to address whether excessive type I IFN signaling neutralizes IL-1 signaling via IL-1Ra in B6.*Sst1*^{S} mice during *Mtb* infection. Accordingly, we crossed B6.*Sst1*^{S} to *Il1rn*$^{-/-}$ mice[58]. Since uninfected *Il1rn*$^{-/-}$

mice exhibit signs of inflammatory disease due to dysregulated IL-1 signaling[54,58,59], and because *Il1rn*$^{+/-}$ mice have a partial decrease in IL-1Ra levels[58], we generated both heterozygous B6.*Sst1*^{S}*Il1rn*$^{+/-}$ and homozygous B6.*Sst1*^{S}*Il1rn*$^{-/-}$ mice. Both heterozygous and homozygous *Il1rn* deficiency protected B6.*Sst1*^{S} mice from *Mtb* (Fig. 4a-d, Extended Data 5a). In fact, bacterial burdens in B6.*Sst1*^{S}*Il1rn*$^{-/-}$ mice were even lower than those found in 'resistant' B6 mice (Fig. 4a). B6.*Sst1*^{S}*Il1rn*$^{-/-}$ mice survived only modestly longer than B6.*Sst1*^{S} mice (Fig. 4b), but this was expected since even uninfected *Il1rn*$^{-/-}$ mice exhibit shortened lifespans due to spontaneous inflammatory disease[59]. Notably, a partial reduction in IL-1Ra levels in heterozygous B6.*Sst1*^{S}*Il1rn*$^{+/-}$ was sufficient to almost entirely reverse the enhanced IFN-driven susceptibility of *Sst1*^{S} mice (Fig. 4a-d). In fact, the bacterial burdens, survival and body weights of B6.*Sst1*^{S}*Il1rn*$^{+/-}$ mice resembled that of B6 mice (Fig. 4a-c, Extended Data 5a). Histological samples of infected lungs showed significant reduction in lesion sizes in both B6.*Sst1*^{S}*Il1rn*$^{+/-}$ and B6.*Sst1*^{S}*Il1rn*$^{-/-}$ mice compared to B6.*Sst1*^{S} (Fig. 4d). Lungs of B6.*Sst1*^{S}*Il1rn*$^{+/-}$ mice infected with a low dose of *Mtb* (~14 CFU) had greater IL-1 bioactivity at day-21 than B6.*Sst1* (Extended Data 5b), but a difference in IL-1 activity was not detectable in mice infected with a higher dose (~55 CFU) (Extended Data 5c), again illustrating the limitations of the IL-1 bioassay as discussed above. Nevertheless, control of the infection in *Il1rn*-deficient mice depended on IL-1 receptor signaling, as B6.*Sst1*^{S}*Il1rn*$^{+/-}$ or B6.*Sst1*^{S}*Il1rn*$^{-/-}$ mice treated with a blocking anti-IL-1R1 antibody[45] exhibited higher bacterial burdens than untreated mice (Extended Data 5e). These data and the known biology of IL-1Ra strongly imply that protection afforded by the loss of IL-1Ra is mediated by enhanced IL-1 signaling, though it is formally possible that *Il1rn* deficiency protects the B6.*Sst1*^{S} mice via a mechanism unrelated to IL-1 and that neutralization of IL-1 signaling dominantly overcomes this protection. Despite decreased bacterial burdens, the lungs of B6.*Sst1*^{S}*Il1rn*$^{+/-}$ mice had similar levels of *Ifnb* or other IFN-induced transcripts as B6.*Sst1*^{S} mice (Extended Data 5d). These results are consistent with a model in which IL-1Ra acts downstream of type I IFN signaling, and does not contribute to reducing *Ifnb* levels other than by reducing overall bacteria burden.

The dramatic protective effects of even partial reductions in IL-1Ra in B6.*Sst1*^{S} mice suggested that IL-1Ra might be a suitable target for host-directed therapy during *Mtb* infection. To test this, we treated infected B6.*Sst1*^{S} mice with an anti-IL-1Ra antibody[60] to block IL-1Ra and restore IL-1 signaling. B6.*Sst1*^{S} mice that received the antibody had significantly lower bacterial burdens in their lungs as compared to PBS-treated controls (Fig. 4e). In addition, mice treated with anti-IL-1Ra antibody retained significantly more body weight than the controls (Fig. 4f) and exhibited reduced lung lesions (Fig. 4g), suggesting that the treatment did not cause detrimental inflammation. To determine if IL-1Ra acts downstream of type I IFN-signaling, we neutralized IL-1Ra in B6.*Sst1*^{S}*Ifnar*$^{-/-}$ mice (Extended Data 5f). Bacterial burdens were similar between B6.*Sst1*^{S}*Ifnar*$^{-/-}$ mice treated with the anti-IL1Ra antibody and control, consistent with the low expression of IL-1Ra in B6.*Sst1*^{S}*Ifnar*$^{-/-}$ mice (Fig. 3c), whereas antibody-treated B6.*Sst1*^{S} mice exhibited reduced CFU. Overall these data indicate that genetic or antibody-mediated reduction of IL-1Ra can rescue the type I IFN-driven susceptibility to tuberculosis in B6.*Sst1*^{S} mice without overt detrimental immunopathology.

The *Sst1* locus spans ~10Mb and encodes ~50 genes. Collectively our data indicate that in B6 (*Sst1*^{R}) mice, the *Sst1* locus acts directly or indirectly to repress type I IFN signaling, though the underlying molecular mechanism is unknown. Previously, *Sst1*^{S} mice were found to lack expression of *Ipr1* (also called *Sp110*) and re-expression of B6-derived *Ipr1*/*Sp110* partially restores resistance to *Mtb*[12]. Thus, loss of *Ipr1*/*Sp110* may account for the *Sst1*^{S} phenotype, though this remains to be confirmed by the generation of B6.*Ipr1*$^{-/-}$ mice. Polymorphisms in human SP110 are associated with TB disease in some but not all cohorts[61-68]. *Ipr1*/*Sp110* is a member of the *Sp100* family of transcriptional regulators that also includes *Sp100*, *Sp140*, and *Aire*. SP100 proteins contain chromatin-binding domains and regulate gene expression. It is tempting to speculate that IPR1/SP110 modulates the chromatin state of type I IFNs and/or IFN-induced genes, though future studies are necessary to establish the molecular basis of the *Sst1*^{S} phenotype.

There is increasing interest in developing host-directed therapeutics for *Mtb*[20]. Although such therapeutics have not yet proven to be curative, and are unlikely to replace antibiotics, they may be advantageous in specific scenarios. For example, host-directed therapy could serve as an adjunct to antibiotics for MDR or XDR-TB, which are associated with high mortality rates[69,70]. If indeed type I IFNs exacerbate TB disease in humans, then a host-directed therapy targeting IL-1Ra, alone or in combination with other host-directed interventions[16], might represent a promising approach. Targeting IL-1Ra may be preferable to blockade of upstream type I IFNs, which might exacerbate viral infections. Regardless, our results show that the B6.*Sst1*^{S} mouse represents a useful model that permits genetic dissection of the molecular mechanisms underlying IFN-driven TB disease.

Methods

Mice.

All mice were specific pathogen-free, maintained under a 12-hr light-dark cycle (7AM to 7PM), and given a standard chow diet (Harlan irradiated laboratory animal diet) *ad libitum*. Within each experiment mice of all genotypes were age-matched at 6-10 weeks old at the beginning of infections. Whenever possible we used comparable numbers of each sex across all genotypes in an experiment. Mice work was not subjected to randomization or data blinding. C57BL/6J (B6), B6.129S-*Il1rn*^{tm1Dih}/J (*Il1rn*$^{-/-}$, Jax #004754)[58], B6(Cg)-*Ifnar1*$^{tm1.2Ees}$/J (*Ifnar*$^{-/-}$, Jax #028288) and B6.129S6-^{Ch25htm1Rus}/J (*Ch25h*$^{-/-}$, JAx #016263)[71] were originally purchased from Jackson Laboratories and subsequently bred at UC Berkeley. B6J.C3-*Sst1*$^{C3HeB/FeJKrmn}$ mice (referred to as B6.*Sst1*^{S} throughout) were from the colony of I. Kramnik at Boston University and then transferred to UC Berkeley. *Sting*$^{gt/gt}$ mice were previously described[72]. All animals used in experiments were bred in-house unless otherwise noted in the figure legends. All animal experiments complied with the regulatory standards of, and were approved by, the University of California Berkeley Institutional Animal Care and Use Committee.

Mycobacterium tuberculosis infections.

Mtb strain Erdman (gift of S.A. Stanley) was used for all infections. Frozen stocks of this wild-type strain were made from a single culture and used for all experiments. Cultures for

infection were grown in Middlebrook 7H9 liquid medium supplemented with 10% albumin-dextrose-saline, 0.4% glycerol and 0.05% Tween-80 for five days at 37°C. Mice were aerosol infected using an inhalation exposure system (Glas-Col, Terre Haute, IN). Cultures were diluted to deliver ~20 to 100 bacteria per mouse as measured by colony forming units (CFUs) in the lungs 1 day following infection, depending on the experiment. Mice were sacrificed at various days post-infection as indicated in the figure legends to measure CFUs and/or cytokines. All but one lung lobe was homogenized in PBS plus 0.05% Tween-80 or processed for cytokines (see below), and serial dilutions were plated on 7H11 plates supplemented with 10% oleic acid, albumin, dextrose, catalase (OADC) and 0.5% glycerol. CFUs were counted 21-25 days after plating. The remaining lobe was used for histology or for RNA extraction. For histology the sample was fixed in 10% formalin for at least 48 hours then stored in 70% ethanol. Samples were sent to Histowiz Inc for embedding in wax, sectioning and hemotoxylin and eosin staining. Samples for RNA were preserved with RNA*later*™ solution (Invitrogen) according to manufacturer specifications for later processing.

Cytokine measurements.

Cell-free lung homogenates were generated as previously described[47]. Briefly, lungs were dissociated through 100μm Falcon cell strainers in sterile PBS with 1% FBS and Pierce Protease Inhibitor EDTA-free (Thermo Fisher). An aliquot was removed for measuring CFU by plating as described above. Cells and debris were then removed by first a low-speed centrifugation (approximately 300×*g*) then a high-speed centrifugation (approximately 2000×*g*) and the resulting cell-free homogenate was filtered twice with 0.2μm filters to remove all *Mtb* for work outside of BSL3. All homogenates were aliquoted, flash-frozen in liquid nitrogen and stored at −80°C. Each aliquot was thawed a maximum of twice to avoid potential artifacts due to repeated freeze-thaw cycles. All cytokines except IL-10 and IL-1Ra was measured using Cytometric Bead Assay (BD Biosciences) according to manufacturer protocols. Results were collected using BD LSRFortessa (BD Biosciences) and analyzed using FCAP Array v3.0. IL-10 levels were measured using Mouse IL-10 ELISA Ready-SET-Go! (2nd Generation, eBioscience). IL-1Ra levels were measured by ELISA using Mouse IL-1ra/IL-1F3 Quantikine ELISA Kit (R&D Systems) according to manufacturer protocols.

IL-1 bioactivity reporter assay.

Mice infected with low dose of *Mtb* (see text for discussion) were used to prepare cell-free lung homogenates. Samples were assayed using HEK-Blue™ IL-1R cells (InvivoGen). Cells were authenticated and tested for mycoplasma by the manufacturer. All experiments use cells under 6 passages from the original stock. 3.75×10^4 cells/well were plated in 96-well plates, and allowed to adhere overnight in DMEM supplemented with 10% FBS, 2mM glutamine, 100U/ml streptomycin and 100μg/ml penicillin. Over-confluence decreases the accuracy of the assay. Cells were treated with 50μl cell-free lung homogenates or standard curve made from recombinant mouse IL-1β (R&D systems 401-ML-005) mixed with 50ul of media overnight. Assays were developed using QUANTI-Blue (InvivoGen) according to manufacturer protocols.

Flow cytometry.

Lungs were perfused with 10 ml of cold PBS and dissociated through 40μm cell strainers. Aliquots were removed for quantifying CFU. Cells were washed and stained with fixable viability dye (Thermo Fisher 65-0865-14). An aliquot of cells from each sample were removed and mixed with counting beads (Thermo Fisher C36950) for later enumeration. The rest of the cells were incubated with anti-mouse CD16/CD32 monoclonal antibody to block Fc receptors (Thermo Fisher 14-0161-81), then with antibodies for surface staining. The following antigens were stained for: CD45 (30-F11, Biolegend 103107), CD11b (M1/70, Thermo Fisher 48-0112-82), CD11c (N418, Biolegend 117335), Ly6G (1A8, BD Biosciences 740554), Ly6C (HK1.4, Thermo Fisher 17-5932-80), CD24 (M1/69, BD Bioscience 564664), MHC II (M5/114.15.2, Biolegend 107625), SiglecF (E50-2440, BD Biosciences 562680). Cells were fixed with fixation buffer (BD Biosciences 554714) for at least 1 hour at room temperature and stored in PBS with 1% FBS and 2mM EDTA overnight at 4°C in the dark. Data were acquired on a BD Fortessa X-20 flow cytometer and analyzed with FlowJo v10.

Bone marrow-derived macrophages (BMMs) and TNF-treatment.

Bone marrow was harvested from mouse femurs and tibias, and cells were differentiated by culture on non-tissue culture-treated plates in RPMI supplemented with supernatant from 3T3-MCSF cells (gift of B. Beutler), 10% fetal bovine serum (FBS), 2mM glutamine, 100 U/ml streptomycin and 100 μg/ml penicillin in a humidified incubator (37°C, 5%CO_2). BMMs were harvested six days after plating and frozen in 95% FBS and 5% DMSO. For *in vitro* experiments, BMMs were thawed into media as described above for 4 hours in a humidified 37°C incubator. Adherent cells were washed with PBS, counted and replated at 1.2×10^6 ~ 1.5×10^6 cells/well in a TC-treated 6-well plate. Cells were treated with 10ng/ml recombinant mouse TNFα (410-TRNC-010, R&D systems) diluted in the media as described above.

Quantitative RT-PCR.

Total RNA from BMMs was extract using RNeasy total RNA kit (Qiagen) according to manufacturer specifications. Total lung RNA was extracted by homogenizing the tissue in TRIzol reagent (Life technologies) then mixing thoroughly with chloroform, both done under BSL3 conditions. Samples were then removed from the BSL3 facility and transferred to fresh tubes under BSL2 conditions. Aqueous phase was separated by centrifugation and RNA was further purified using an RNeasy total RNA kit (Qiagen). Equal amounts of RNA from each sample were treated with DNase (RQ1, Promega) and cDNA was made using Superscript III (Invitrogen). Complementary cDNA reactions were primed with poly(dT) for the measurement of mature transcripts. Quantitative PCR was performed using QuantiStudio 5 Real-Time PCR System (Applied Biosystems) with Power Sybr Green PCR Master Mix (Thermo Fisher Scientific) according manufacturer specifications. Transcript levels were normalized to housekeeping genes *Rps17, Actb and Oaz1* unless otherwise specified. The following primers were used in this study. *Rps17* sense: CGCCATTATCCC CAGCAAG; *Rps17* antisense: TGTCGGGATCCACCTCAATG; *Oaz1* sense: GTGGTGGCCTCTACATCGAG; *Oaz1* antisense: AGCAGATGAAAACGTGGTCAG;

Actb sense: CGCAGCCACTGTCGAGTC; *Actb* antisense: CCTTCTGACCCATTCCCACC; *Ifnb* sense: GTCCTCAACTGCTCTCCACT; *Ifnb* antisense: CCTGCAACCACCACTCATTC; *Il1rn* sense: CGCCCTTCTGGGAAAAGACC, *Il1rn* antisense: CCGTGGATGCCCAAGAACAC; *Gbp5* sense: TGTTCTTACTGGCCCCTGCT; *Gbp5* antisense: CCAATGAGGCACAAGGGTTC; *Ifit3* sense: AGCCCACACCCAGCTTTT; *Ifit3* antisense: CAGAGATTCCCGGTTGACCT; *Ch25h* sense: CACTCGGGCTATGACTTCCC; *Ch25h* antisense: GAGTGCCCAGCATTTTGTCC; *Irf1* sense: TGAGGAAGGGAAGATAGCCG; *Irf1* antisense: TGTATGCCTATCCCAATGTCCC; *Irgm1* sense: AAAACCAGAGAGCCTCACCA;
Irgm1 antisense: ATGTTGGGGAGTAGTGGAGC; *Gbp4* sense: TGAGTACCTGGAGAATGCCCT; *Gbp4* antisense: TGGCCGAATTGGATGCTTGG; *Stat1* sense: CAGAAAAACGCTGGGAACAGA; *Stat1* antisense: CAAGCCTGGCTGGCAC; *Gbp7* sense: AGCAAGCCCAAGTTCACACT; *Gbp7* antisense: TCCGCTCTGTCAGTTCTGTG.

Antibody-mediated neutralization.

For all antibody treatments, the schedules are indicated in the figures. All treatments were delivered by intraperitoneal injection. Mouse anti-mouse IFNAR1 (MAR1-5A3) and isotype control (GIR208, mouse anti-human IFNGR-α chain) were purchased from Leinco Technologies Inc. Each mouse was given 500μg per injection. Hamster anti-IL-1R1 antibody (mIL1R-M147) was obtained from Amgen[45]. Isotype control was Ultra-LEAF Purified Armenian Hamster IgG Isotype Antibody from Biolegend (400940). Each mouse was given 200μg per injection. Armenian hamster anti-IL1Ra antibody was produced in-house using a previously published hybridoma line[60]. Cells were grown in Wheaton CELLine Bioreactor Flasks (Fisher Scientific) according to manufacturer instructions. Media in the cell compartment used ultra-low IgG FBS (ThermoFisher 16250078) to minimize bovine IgG contamination during purification. Cell-free supernatant from the cell compartment was purified using protein G resin (GenScript). IgG was eluted using 0.1M acetic acid, then 10% of total volume of 1M Tris pH8 and 0.5M NaCl was added to neutralize. Size exclusion and buffer exchange to PBS was performed using Amicon Ultra-4 Centrifugal Filter Units (EMD Millipore). The final product was filter sterilized and stored at −80°C. For injections antibody stocks were diluted in sterile PBS and each mouse received 500μg per injection.

Statistical analysis.

All survival data were analyzed with two-ended Log-rank test. All other data were analyzed with two-ended Mann-Whitney test unless otherwise noted. Both tests were run using GraphPad Prism 5. Asterisk, $p \leq 0.05$; two asterisks, $p \leq 0.01$; three asterisks, $p \leq 0.001$. All error bars are SEM and all center bars indicate means.

Extended Data

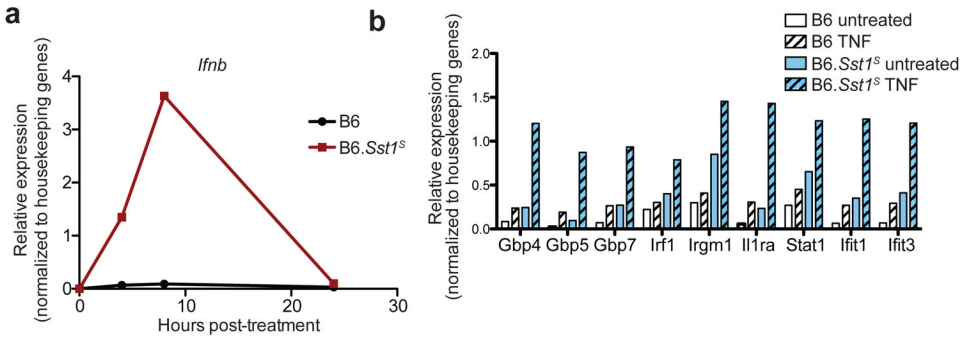

Extended Data 1 |. B6.*Sst1*^{S} BMMs overexpress *Ifnb* and ISGs when stimulated with TNFα.
a-b, Expression of *Ifnb* (**a**) or selected ISGs (**b**) in BMMs measured by RT-qPCR. Results normalized to housekeeping genes. Representative data of at least two independent experiments.

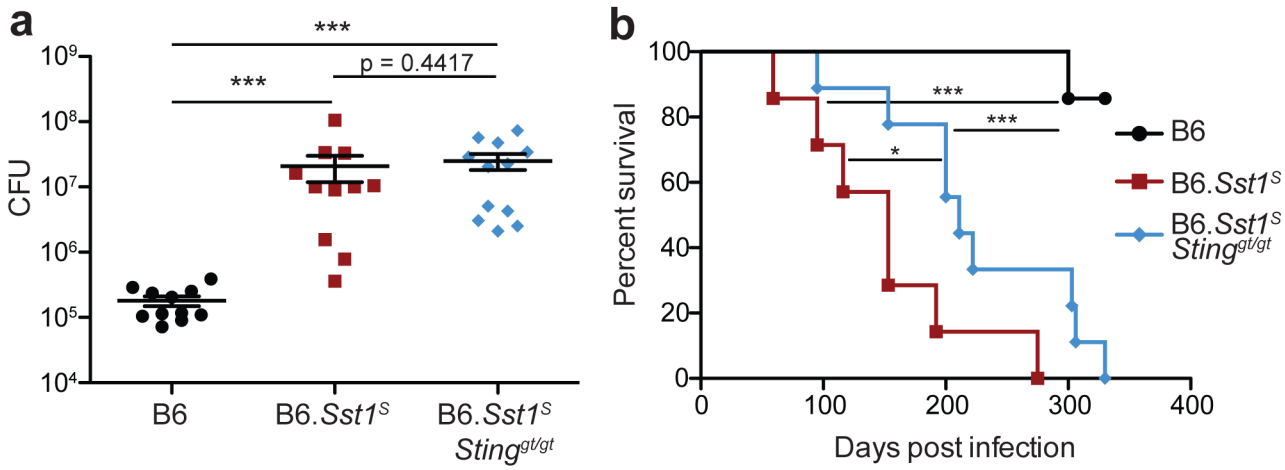

Extended Data 2 |. B6.*Sst1*^{S}*Sting*$^{gt/gt}$ partially rescues the enhance susceptibility of B6.*Sst1*^{S} mice to *Mtb*.

Mice were infected with *Mtb* and measured for lung bacterial burdens at day 25 (**a**) or survival (**b**). **a**, combined results of 2 experiments. Sample size n (B6, B6.*Sst1*^{S}, B6.*Sst1*^{S}*Sting*$^{gt/gt}$) = 11, 11, 12 (**a**); 11, 11, 11 (**b**). All animals except 5 of the B6 were bred in-house (**a**) and all except B6 were bred in-house (**b**). Center and error bars show mean and SEM. Analyzed with two-ended Mann-Whitney test (**a**) or two-ended Log-rank test (**b**). *$P \leq 0.05$; **$P \leq 0.01$; ***$P \leq 0.001$.

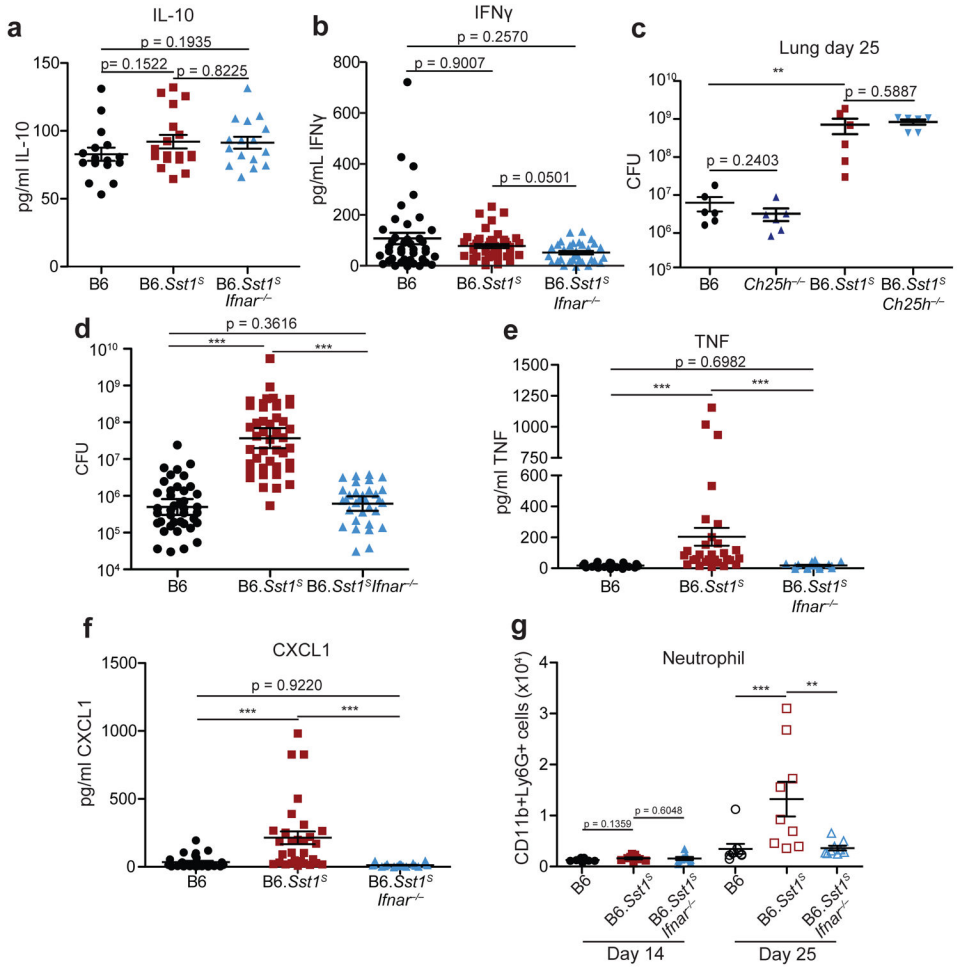

Extended Data 3 |. Enhanced inflammation in B6.*Sst1*^{S} mice requires type I IFN.

a, b, e, f, Protein levels of IL-10 (**a**), IFNγ (**b**), TNF (**e**), and CXCL1 (**f**) were measured in lungs of *Mtb*-infected mice at day 25. Combined results of at least three independent infections (**a**, **b**, **e**, **f**). **c**, Lung bacterial burden of *Mtb*-infected mice at day 25 (representative of two independent infections). Input dose: average 100CFU/mouse. **d**, CFU corresponding to Figure 2a and b. Combined results that include those already shown in Figures 1c, 2c, and Extended Data 3a. Input dose: average 10-89CFU/mouse. **g**, Neutrophils (CD11b+Ly6G+) from lungs of *Mtb*-infected mice were enumerated on day 14 and day 25. Combined results of two independent infections. All animals except B6 were bred in-house (**a**-**f**); all animals were bred in-house (**g**). Sample size *n* (B6, B6.*Sst1*^{S}, B6.*Sst1*^{S}*Ifnar*$^{-/-}$) = 16, 18, 16 (**a**); 40, 45, 32 (**b**); 40, 44, 32 (**d**); 25, 29, 16 (**e**); 28, 30, 26 (**f**); 6 for all genotypes (**c**); 9 for all genotypes (**g**). Center and error bars show mean and SEM. Analyzed with two-ended Mann-Whitney test (**a**-**g**). *$P \leq 0.05$; **$P \leq 0.01$; ***$P \leq 0.001$

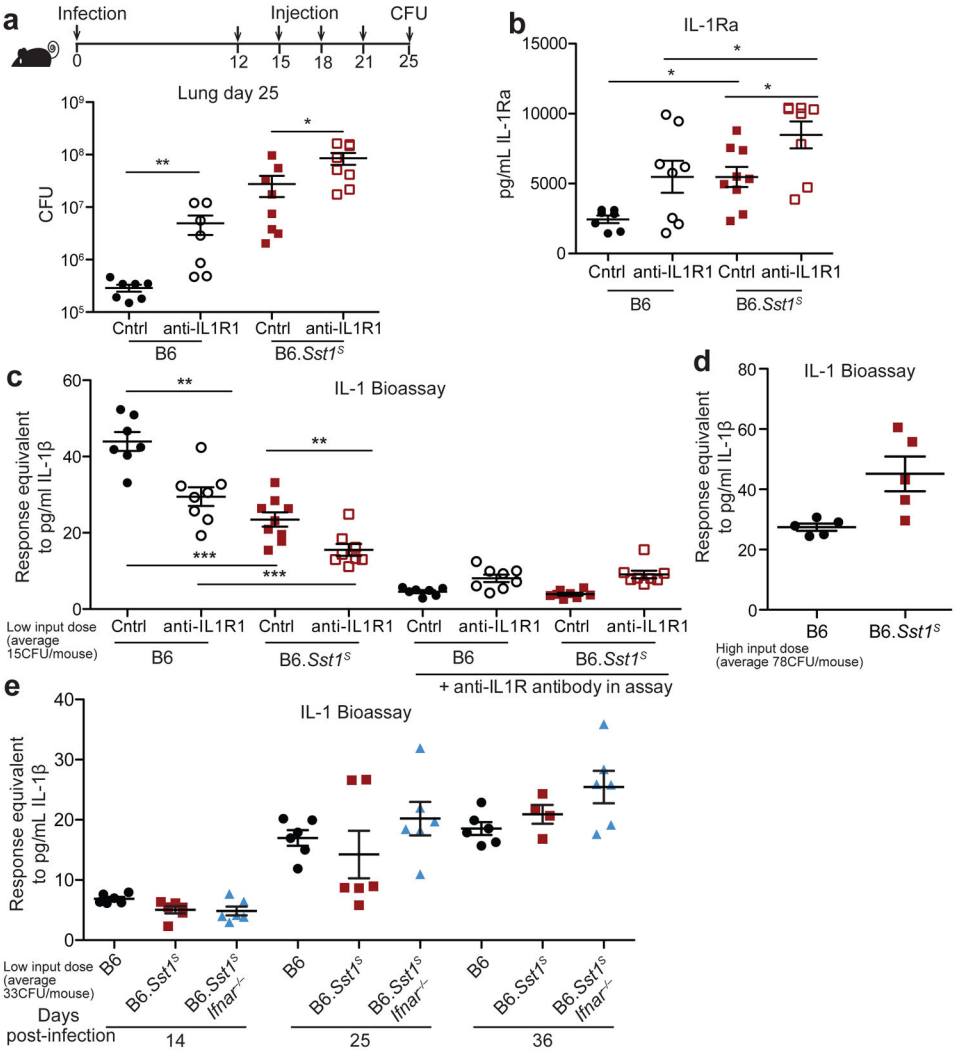

Extended Data 4 |. IL-1 blockade increases susceptibility in both B6 and B6.*Sst1*^{S} mice.

a-c, mice were infected with average 15CFU/mouse and were treated with anti-IL1R1 or isotype control antibodies, and on day 25 the lungs were measured for bacterial burden (**a**), IL-1Ra protein levels (**b**), and IL-1 bioactivity (**c**). Sample size n (in order shown, from left) = 7, 7, 8, 8 (**a**); 7, 8, 9, 8 (**b-c**). **d**, Mice were infected with average 78CFU/mouse and IL-1 bioactivity was measured in the lungs at day 25. n = 5 for both samples. **e**, Mice were infected with average 33CFU/mouse. IL-1 bioactivity was measured in lung samples collected on the indicated days. n = 6 for all samples except day 36 B6.*Sst1*^{S} = 4. Day 25 data already shown in Fig. 3d. All animals except B6 were bred in-house (**a-c**); all were bred in-house (**d-e**). Center and error bars show mean and SEM. Analyzed with two-ended Mann-Whitney test (**a-c**). *$P \leq 0.05$; **$P \leq 0.01$; ***$P \leq 0.001$.

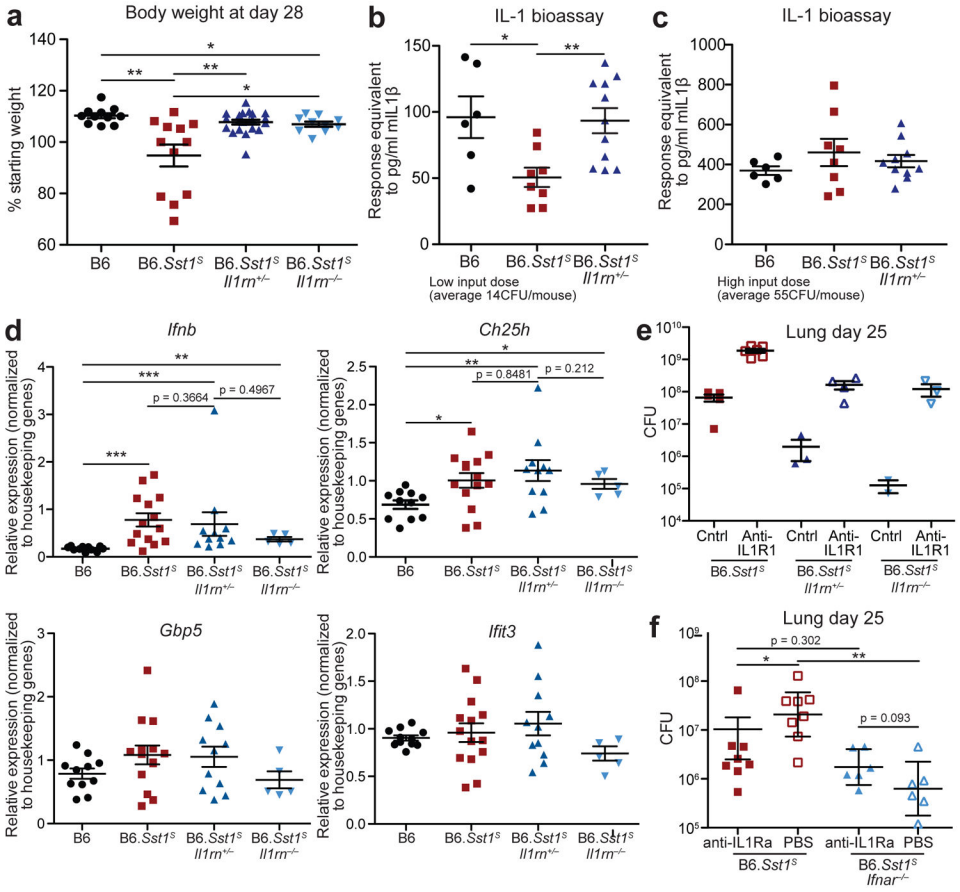

Extended Data 5 |. Homozygous or heterozygous *Il1rn* deletion protects B6.*Sst1*^{S} mice from *Mtb* infection.

a, Body weights on day 28 of individual mice shown in Fig. 4c. **b**-**c**, Mice were infected with *Mtb* at average 14CFU/mouse (**b**) or 55CFU/mouse (**c**), and at day 21 lungs were harvested to measure IL-1 bioactivity. **d**, RT-qPCR on lungs of *Mtb*-infected mice, sampled at 25 days post-infection. Each graph combined results from 2 independent experiments. **e**-**f**, Mice infected with average 20 CFU/mouse were treated with either anti-IL-1R1 antibody or isotype control every 3 days starting 7 days post-infection (**e**), or anti-IL-1Ra antibody or PBS control every other day starting 3 days post-infection (**f**). At 25 days post-infection lungs were harvested for measuring bacterial burden. Sample size n (from left as shown) = 11, 12, 22, 10(**a**); 6, 8, 11(**b**); 6, 8, 10(**c**); 11, 14, 11, 5(**d**); 5, 6, 3, 4, 2, 3(**e**); 8, 8, 6, 6(**f**). All mice were bred in-house (**a**, **d**-**f**) or all except B6 were bred in-house (**b**-**c**); and all except B6 and B6.*Sst1*^{S} were littermates (**a**, **d**, **e**). Center and error bars show mean and SEM. Analyzed with two-ended Mann-Whitney test. *$P \leq 0.05$; **$P \leq 0.01$; ***$P \leq 0.001$.

Acknowledgements

We thank the Stanley and Cox labs for discussions and for support with *Mtb* experiments, L. Flores, P. Dietzen and R. Chavez for technical assistance, H. Nolla and A. Valeros and the Cancer Research Laboratory for flow cytometry. We thank the Barton lab, I. Rauch, A. Sandstrom, D. Kotov, and P. Mitchell for helpful discussions and technical support. We thank B. Penn for comments on the manuscript. Generation of the anti-IL1Ra antibody was supported by the Extramural Collaborative Research Program of Cancer Research Institute, Kanazawa University. K.H.D and R.E.V. were supported by Investigator in the Pathogenesis of Infectious Diseases awards from the

Burroughs Wellcome Fund. R.E.V. is an HHMI Investigator and is supported by NIH grants AI075039 and AI066302.

References

1. World Health Organization. Global Tuberculosis Report 2018. (2018).
2. Zak DE et al. A blood RNA signature for tuberculosis disease risk: a prospective cohort study. Lancet 387, 2312–2322 (2016). [PubMed: 27017310]
3. Scriba TJ et al. Sequential inflammatory processes define human progression from M. tuberculosis infection to tuberculosis disease. PLoS Pathog. 13, e1006687 (2017). [PubMed: 29145483]
4. Berry MPR et al. An interferon-inducible neutrophil-driven blood transcriptional signature in human tuberculosis. Nature 466, 973–7 (2010). [PubMed: 20725040]
5. Singhania A et al. A modular transcriptional signature identifies phenotypic heterogeneity of human tuberculosis infection. Nat. Commun 9, 2308 (2018). [PubMed: 29921861]
6. Moreira-Teixeira L, Mayer-Barber K, Sher A & O'Garra A Type I interferons in tuberculosis: Foe and occasionally friend. J. Exp. Med 215, 1273–1285 (2018). [PubMed: 29666166]
7. Donovan ML, Schultz TE, Duke TJ & Blumenthal A Type I Interferons in the Pathogenesis of Tuberculosis: Molecular Drivers and Immunological Consequences. Front. Immunol 8, 1633 (2017). [PubMed: 29230217]
8. Stanley SA, Johndrow JE, Manzanillo P & Cox JS The Type I IFN response to infection with Mycobacterium tuberculosis requires ESX-1-mediated secretion and contributes to pathogenesis. J. Immunol 178, 3143–52 (2007). [PubMed: 17312162]
9. Antonelli LRV et al. Intranasal Poly-IC treatment exacerbates tuberculosis in mice through the pulmonary recruitment of a pathogen-permissive monocyte/macrophage population. J. Clin. Invest 120, 1674–82 (2010). [PubMed: 20389020]
10. Desvignes L, Wolf AJ & Ernst JD Dynamic Roles of Type I and Type II IFNs in Early Infection with Mycobacterium tuberculosis. J. Immunol 188, 6205–6215 (2012). [PubMed: 22566567]
11. Moreira-Teixeira L et al. Type I IFN Inhibits Alternative Macrophage Activation during Mycobacterium tuberculosis Infection and Leads to Enhanced Protection in the Absence of IFN-γ Signaling. J. Immunol 197, 4714–4726 (2016). [PubMed: 27849167]
12. Pan H et al. Ipr1 gene mediates innate immunity to tuberculosis. Nature 434, 767–72 (2005). [PubMed: 15815631]
13. Pichugin AV, Yan BS, Sloutsky A, Kobzik L & Kramnik I Dominant role of the sst1 locus in pathogenesis of necrotizing lung granulomas during chronic tuberculosis infection and reactivation in genetically resistant hosts. Am. J. Pathol 174, 2190–2201 (2009). [PubMed: 19443700]
14. Kramnik I, Dietrich WF, Demant P & Bloom BR Genetic control of resistance to experimental infection with virulent Mycobacterium tuberculosis. Proc. Natl. Acad. Sci 97, 8560–8565 (2002).
15. Mayer-Barber KD et al. Innate and Adaptive Interferons Suppress IL-1α and IL-1β Production by Distinct Pulmonary Myeloid Subsets during Mycobacterium tuberculosis Infection. Immunity 35, 1023–1034 (2011). [PubMed: 22195750]
16. Mayer-Barber KD et al. Host-directed therapy of tuberculosis based on interleukin-1 and type I interferon crosstalk. Nature 511, 99–103 (2014). [PubMed: 24990750]
17. McNab FW et al. Type I IFN induces IL-10 production in an IL-27-independent manner and blocks responsiveness to IFN-γ for production of IL-12 and bacterial killing in Mycobacterium tuberculosis-infected macrophages. J. Immunol 193, 3600–12 (2014). [PubMed: 25187652]
18. Boxx GM & Cheng G The Roles of Type I Interferon in Bacterial Infection. Cell Host Microbe 19, 760–769 (2016). [PubMed: 27281568]
19. Nunes-Alves C et al. In search of a new paradigm for protective immunity to TB. Nat. Rev. Microbiol 12, 289–299 (2014). [PubMed: 24590243]
20. Hawn TR, Shah JA & Kalman D New tricks for old dogs: Countering antibiotic resistance in tuberculosis with host-directed therapeutics. Immunol. Rev 264, 344–362 (2015). [PubMed: 25703571]
21. Zhang G et al. A proline deletion in IFNAR1 impairs IFN-signaling and underlies increased resistance to tuberculosis in humans. Nat. Commun 9, 85 (2018). [PubMed: 29311663]

22. de Oliveira Uehara SN et al. High incidence of tuberculosis in patients treated for hepatitis C chronic infection. Brazilian J. Infect. Dis 20, 205–9 (2016).
23. Matsuoka S et al. Onset of Tuberculosis from a Pulmonary Latent Tuberculosis Infection during Antiviral Triple Therapy for Chronic Hepatitis C. Intern. Med 55, 2011–7 (2016). [PubMed: 27477407]
24. Sabbatani S et al. Reactivation of severe, acute pulmonary tuberculosis during treatment with pegylated interferon-alpha and ribavirin for chronic HCV hepatitis. Scand. J. Infect. Dis 38, 205–8 (2006). [PubMed: 16500782]
25. Manca C et al. Virulence of a Mycobacterium tuberculosis clinical isolate in mice is determined by failure to induce Th1 type immunity and is associated with induction of IFN-alpha /beta. Proc. Natl. Acad. Sci 98, 5752–7 (2001). [PubMed: 11320211]
26. Dorhoi A et al. Type I IFN signaling triggers immunopathology in tuberculosis-susceptible mice by modulating lung phagocyte dynamics. Eur. J. Immunol 44, 2380–2393 (2014). [PubMed: 24782112]
27. Teles RMB et al. Type I interferon suppresses type II interferon-triggered human anti-mycobacterial responses. Science (80-.). 339, 1448–53 (2013).
28. McNab F, Mayer-Barber K, Sher A, Wack A & O'Garra A Type I interferons in infectious disease. Nat. Rev. Immunol 15, 87–103 (2015). [PubMed: 25614319]
29. Bhattacharya B et al. The integrated stress response mediates type I interferon driven necrosis in Mycobacterium tuberculosis granulomas. bioRxiv (2018).
30. He X et al. The sst1 resistance locus regulates evasion of type I interferon signaling by Chlamydia pneumoniae as a disease tolerance mechanism. PLoS Pathog. 9, e1003569 (2013). [PubMed: 24009502]
31. Dunn GP et al. A critical function for type I interferons in cancer immunoediting. Nat. Immunol 6, 722–729 (2005). [PubMed: 15951814]
32. Watson RO et al. The Cytosolic Sensor cGAS Detects Mycobacterium tuberculosis DNA to Induce Type I Interferons and Activate Autophagy. Cell Host Microbe 17, 811–819 (2015). [PubMed: 26048136]
33. Wassermann R et al. Mycobacterium tuberculosis Differentially Activates cGAS- and Inflammasome-Dependent Intracellular Immune Responses through ESX-1. Cell Host Microbe 17, 799–810 (2015). [PubMed: 26048138]
34. Wiens KE & Ernst JD The Mechanism for Type I Interferon Induction by Mycobacterium tuberculosis is Bacterial Strain-Dependent. PLoS Pathog. 12, 1–20 (2016).
35. Dey B et al. A bacterial cyclic dinucleotide activates the cytosolic surveillance pathway and mediates innate resistance to tuberculosis. Nat. Med 21, 401–408 (2015). [PubMed: 25730264]
36. Collins AC et al. Cyclic GMP-AMP Synthase Is an Innate Immune DNA Sensor for Mycobacterium tuberculosis. Cell Host Microbe 17, 820–828 (2015). [PubMed: 26048137]
37. Manzanillo PS, Shiloh MU, Portnoy DA & Cox JS Mycobacterium tuberculosis activates the DNA-dependent cytosolic surveillance pathway within macrophages. Cell Host Microbe 11, 469–480 (2012). [PubMed: 22607800]
38. Eshleman EM, Delgado C, Kearney SJ, Friedman RS & Lenz LL Down regulation of macrophage IFNGR1 exacerbates systemic L. monocytogenes infection. PLoS Pathog. 13, 1–22 (2017).
39. Rayamajhi M, Humann J, Penheiter K, Andreasen K & Lenz LL Induction of IFN-alphabeta enables Listeria monocytogenes to suppress macrophage activation by IFN-gamma. J. Exp. Med 207, 327–37 (2010). [PubMed: 20123961]
40. Reboldi A et al. 25-Hydroxycholesterol suppresses interleukin-1-driven inflammation downstream of type I interferon. Science (80-.). 345, 679–84 (2014).
41. Novikov A et al. Mycobacterium tuberculosis triggers host type I IFN signaling to regulate IL-1β production in human macrophages. J. Immunol 187, 2540–7 (2011). [PubMed: 21784976]
42. Mayer-Barber KD & Yan B Clash of the Cytokine Titans: Counter-regulation of interleukin-1 and type I interferon-mediated inflammatory responses. Cell. Mol. Immunol 14, 22–35 (2017). [PubMed: 27264686]

43. Mishra BB et al. Nitric oxide controls the immunopathology of tuberculosis by inhibiting NLRP3 inflammasome-dependent processing of IL-1β. Nat. Immunol 14, 52–60 (2013). [PubMed: 23160153]
44. Mishra BB et al. Nitric oxide prevents a pathogen-permissive granulocytic inflammation during tuberculosis. Nat. Microbiol 2, 17072 (2017). [PubMed: 28504669]
45. Nichols RD, Von Moltke J & Vance RE NAIP/NLRC4 inflammasome activation in MRP8+ cells is sufficient to cause systemic inflammatory disease. Nat. Commun 8, (2017).
46. Fremond CM et al. IL-1 receptor-mediated signal is an essential component of MyD88-dependent innate response to Mycobacterium tuberculosis infection. J. Immunol 179, 1178–89 (2007). [PubMed: 17617611]
47. Mayer-Barber KD et al. Caspase-1 independent IL-1beta production is critical for host resistance to Mycobacterium tuberculosis and does not require TLR signaling in vivo. J. Immunol 184, 3326–30 (2010). [PubMed: 20200276]
48. Yamada H, Mizumo S, Horai R, Iwakura Y & Sugawara I Protective role of interleukin-1 in mycobacterial infection in IL-1 alpha/beta double-knockout mice. Lab. Invest 80, 759–67 (2000). [PubMed: 10830786]
49. Sugawara I, Yamada H, Hua S & Mizuno S Role of interleukin (IL)-1 type 1 receptor in mycobacterial infection. Microbiol. Immunol 45, 743–750 (2001). [PubMed: 11791667]
50. Di Paolo NC et al. Interdependence between Interleukin-1 and Tumor Necrosis Factor Regulates TNF-Dependent Control of Mycobacterium tuberculosis Infection. Immunity 43, 1125–1136 (2015). [PubMed: 26682985]
51. Juffermans NP et al. Interleukin-1 Signaling Is Essential for Host Defense during Murine Pulmonary Tuberculosis. J. Infect. Dis 182, 902–908 (2002).
52. Bohrer AC, Tocheny C, Assmann M, Ganusov VV & Mayer-Barber KD Cutting Edge: IL-1R1 Mediates Host Resistance to Mycobacterium tuberculosis by Trans-Protection of Infected Cells. J. Immunol 201, 1645–1650 (2018). [PubMed: 30068597]
53. Eisenberg SP et al. Primary structure and functional expression from complementary DNA of a human interleukin-1 receptor antagonist. Nature 343, 341–6 (1990). [PubMed: 2137201]
54. Dinarello CA Overview of the IL-1 family in innate inflammation and acquired immunity. Immunol. Rev 281, 8–27 (2018). [PubMed: 29247995]
55. Molnarfi N, Hyka-Nouspikel N, Gruaz L, Dayer J-M & Burger D The production of IL-1 receptor antagonist in IFN-beta-stimulated human monocytes depends on the activation of phosphatidylinositol 3-kinase but not of STAT1. J. Immunol 174, 2974–80 (2005). [PubMed: 15728510]
56. Corr M et al. Interleukin 1 receptor antagonist mediates the beneficial effects of systemic interferon beta in mice: Implications for rheumatoid arthritis. Ann. Rheum. Dis 70, 858–863 (2011). [PubMed: 21216819]
57. Cohen SB et al. Alveolar Macrophages Provide an Early Mycobacterium tuberculosis Niche and Initiate Dissemination. Cell Host Microbe 24, 439–446.e4 (2018). [PubMed: 30146391]
58. Hirsch E, Irikura VM, Paul SM & Hirsh D Functions of interleukin 1 receptor antagonist in gene knockout and overproducing mice. Proc. Natl. Acad. Sci 93, 11008–11013 (2002).
59. Nicklin MJH, Hughes DE, Barton JL, Ure JM & Duff GW Arterial inflammation in mice lacking the interleukin 1 receptor antagonist gene. J. Exp. Med 191, 303–12 (2000). [PubMed: 10637274]
60. Fujioka N et al. Preparation of specific antibodies against murine IL-1ra and the establishment of IL-1ra as an endogenous regulator of bacteria-induced fulminant hepatitis in mice. J. Leukoc. Biol 58, 90–98 (1995). [PubMed: 7616110]
61. Lei X, Zhu H, Zha L & Wang Y SP110 gene polymorphisms and tuberculosis susceptibility: A systematic review and meta-analysis based on 10 624 subjects. Infect. Genet. Evol 12, 1473–1480 (2012). [PubMed: 22691368]
62. Cai L et al. Identification of genetic associations of SP110/MYBBP1A/RELA with pulmonary tuberculosis in the Chinese Han population. Hum. Genet 132, 265–73 (2013). [PubMed: 23129390]
63. Fox GJ et al. Polymorphisms of SP110 are associated with both pulmonary and extra-pulmonary tuberculosis among the Vietnamese. PLoS One 9, e99496 (2014). [PubMed: 25006821]

64. Ren G et al. SP110 and PMP22 polymorphisms are associated with tuberculosis risk in a Chinese-Tibetan population. Oncotarget 7, 66100–66108 (2016). [PubMed: 27623071]

65. Leu JS et al. SP110b controls host immunity and susceptibility to tuberculosis. Am. J. Respir. Crit. Care Med 195, 369–382 (2017). [PubMed: 27858493]

66. Zhang S et al. Certain Polymorphisms in SP110 Gene Confer Susceptibility to Tuberculosis: A Comprehensive Review and Updated Meta-Analysis. Yonsei Med. J 58, 165–173 (2017). [PubMed: 27873510]

67. Zhou Y et al. Polymorphisms in the SP110 and TNF-α Gene and Susceptibility to Pulmonary and Spinal Tuberculosis among Southern Chinese Population. Dis. Markers 2017, 4590235 (2017). [PubMed: 29430075]

68. Chang S-Y et al. SP110 Polymorphisms Are Genetic Markers for Vulnerability to Latent and Active Tuberculosis Infection in Taiwan. Dis. Markers 2018, 4687380 (2018). [PubMed: 30627224]

69. Mitnick CD et al. Aggressive regimens for multidrug-resistant tuberculosis decrease all-cause mortality. PLoS One 8, e58664 (2013). [PubMed: 23516529]

70. Chung-Delgado K, Guillen-Bravo S, Revilla-Montag A & Bernabe-Ortiz A Mortality among MDR-TB cases: comparison with drug-susceptible tuberculosis and associated factors. PLoS One 10, e0119332 (2015). [PubMed: 25790076]

71. Bauman DR et al. 25-Hydroxycholesterol secreted by macrophages in response to Toll-like receptor activation suppresses immunoglobulin A production. Proc. Natl. Acad. Sci 106, 16764–16769 (2009). [PubMed: 19805370]

72. Sauer J-D et al. The N-ethyl-N-nitrosourea-induced Goldenticket mouse mutant reveals an essential function of Sting in the in vivo interferon response to Listeria monocytogenes and cyclic dinucleotides. Infect. Immun 79, 688–94 (2011). [PubMed: 21098106]

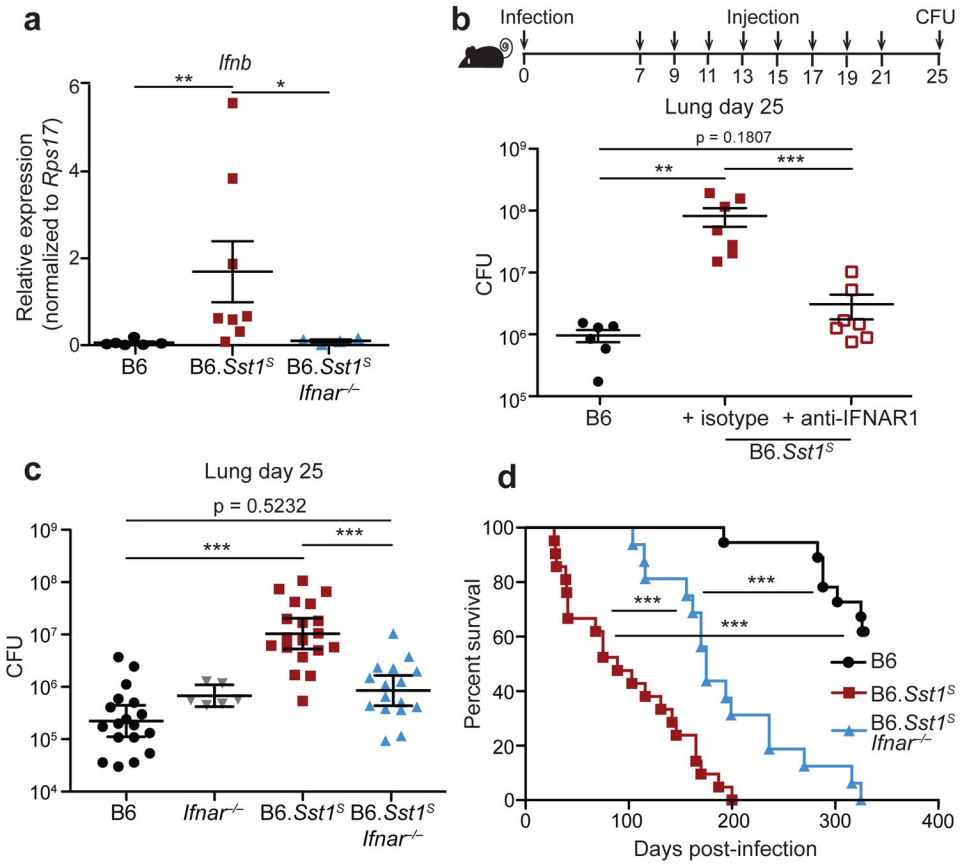

Fig. 1 |. Type I IFN drives enhanced susceptibility of B6.*Sst1*^{S} mice.

a, Expression of *Ifnb* in *Mtb*-infected lungs at day 25, measured by quantitative RT-PCR, normalized to *Rps17*. **b**, Lung bacterial burdens at day 25 from *Mtb*-infected mice treated with anti-IFNAR1 or isotype control antibody. **c**, Lung bacterial burdens at day 25, or **d**, survival, of *Mtb*-infected mice. **c**-**d**, Combined results from three independent infections. Sample size n: B6 = 6, B6.*Sst1*^{S} = 8, B6.*Sst1*^{S}*Ifnar*$^{-/-}$ = 4 (**a**); B6 = 6, isotype = 7, anti-IFNAR1 = 7 (**b**); B6 = 18, *Ifnar*$^{-/-}$ = 6, B6.*Sst1*^{S} = 19, B6.*Sst1*^{S}*Ifnar*$^{-/-}$ = 16 (**c**); B6 = 18, B6.*Sst1*^{S} = 21, B6.*Sst1*^{S}*Ifnar*$^{-/-}$ = 16 (**d**). For **a**-**d**, all except B6 mice were bred in-house. Center and error bars show mean and SEM. Analyzed with two-ended Mann-Whitney test (**a**-**c**) or two-ended Log-rank test (**d**). Asterisk, $p \leq 0.05$; two asterisks, $p \leq 0.01$; three asterisks, $p \leq 0.001$.

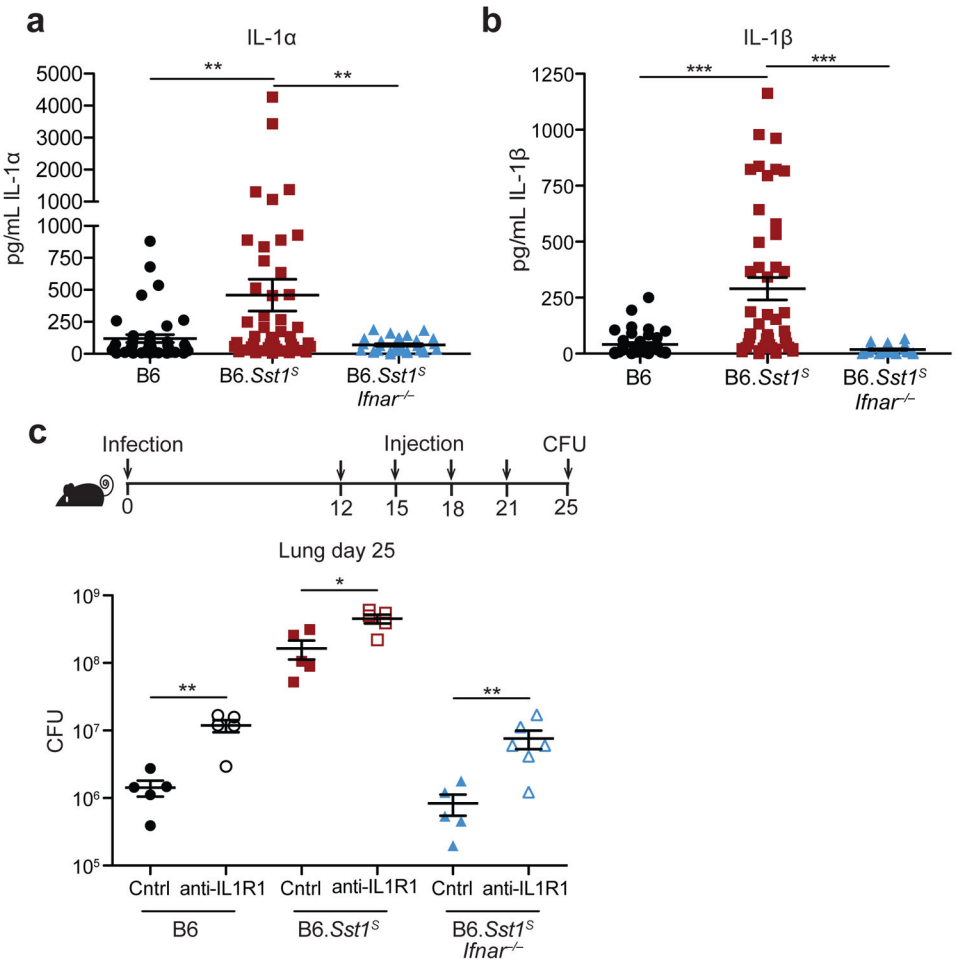

Fig. 2 | IFNAR signaling results in high but non-pathological IL-1 protein levels in B6.*Sst1*^{S} mice.

a-b, Protein levels of IL-1α (**a**) and IL-1β (**b**) were measured in the lungs of *Mtb*-infected mice at day 25. Combined results of four independent experiments. n: B6 = 41, B6.*Sst1*^{S} = 46, B6.*Sst1*^{S}*Ifnar*$^{-/-}$ = 33 (**a-b**). **c**, Lung bacterial burdens at day 25 from *Mtb*-infected mice treated with anti-IL1R1 or isotype control antibody. n (from left as shown) =5, 5, 5, 5, 5, 6. All animals except B6 were bred in-house (**a-c**). Center and error bars show mean and SEM. Analyzed with two-ended Mann-Whitney test (**a-c**). Asterisk, $p \leq 0.05$; two asterisks, $p \leq 0.01$; three asterisks, $p \leq 0.001$.

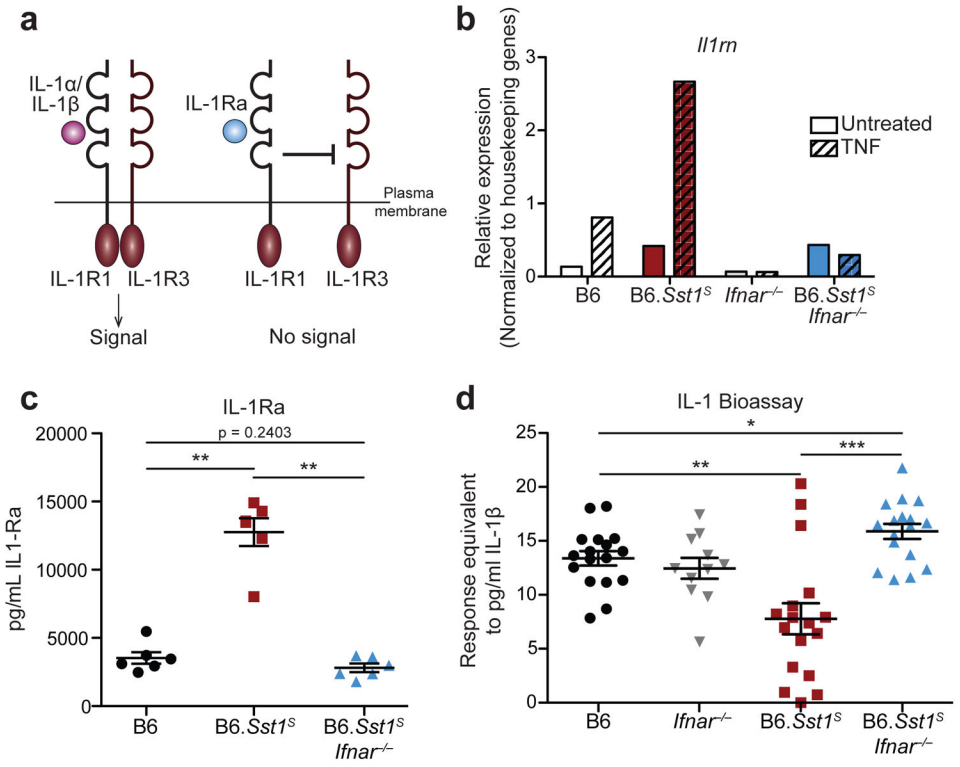

Fig. 3 |. Elevated IL-1Ra and decreased functional IL-1 signaling in *Mtb*-infected B6.*Sst1*^{S} mice.

a, Schematic of IL-1R signaling. **b**, *Il1rn* expression in BMMs treated with 10 ng/ml TNFα for 24 hours. **c**, IL-1Ra protein levels and **d**, IL-1 reporter assay measuring functional IL-1 activity in lungs of *Mtb*-infected mice at day 25. Sample size n: B6 = 6, B6.*Sst1*^{S} = 6, B6.*Sst1*^{S}*Ifnar*$^{-/-}$ = 6 (**c**); B6 = 17, *Ifnar*$^{-/-}$ = 11, B6.*Sst1*^{S} = 17, B6.*Sst1*^{S}*Ifnar*$^{-/-}$ = 17 (**d**). Combined results of three independent infections (**d**) or representative of at least two independent experiments (**b**, **c**). All animals except B6 were bred in-house (**c**-**d**). Center and error bars show mean and SEM (**c**, **d**). Analyzed with two-ended Mann-Whitney test (**c**, **d**). Asterisk, $p \leq 0.05$; two asterisks, $p \leq 0.01$; three asterisks, $p \leq 0.001$.

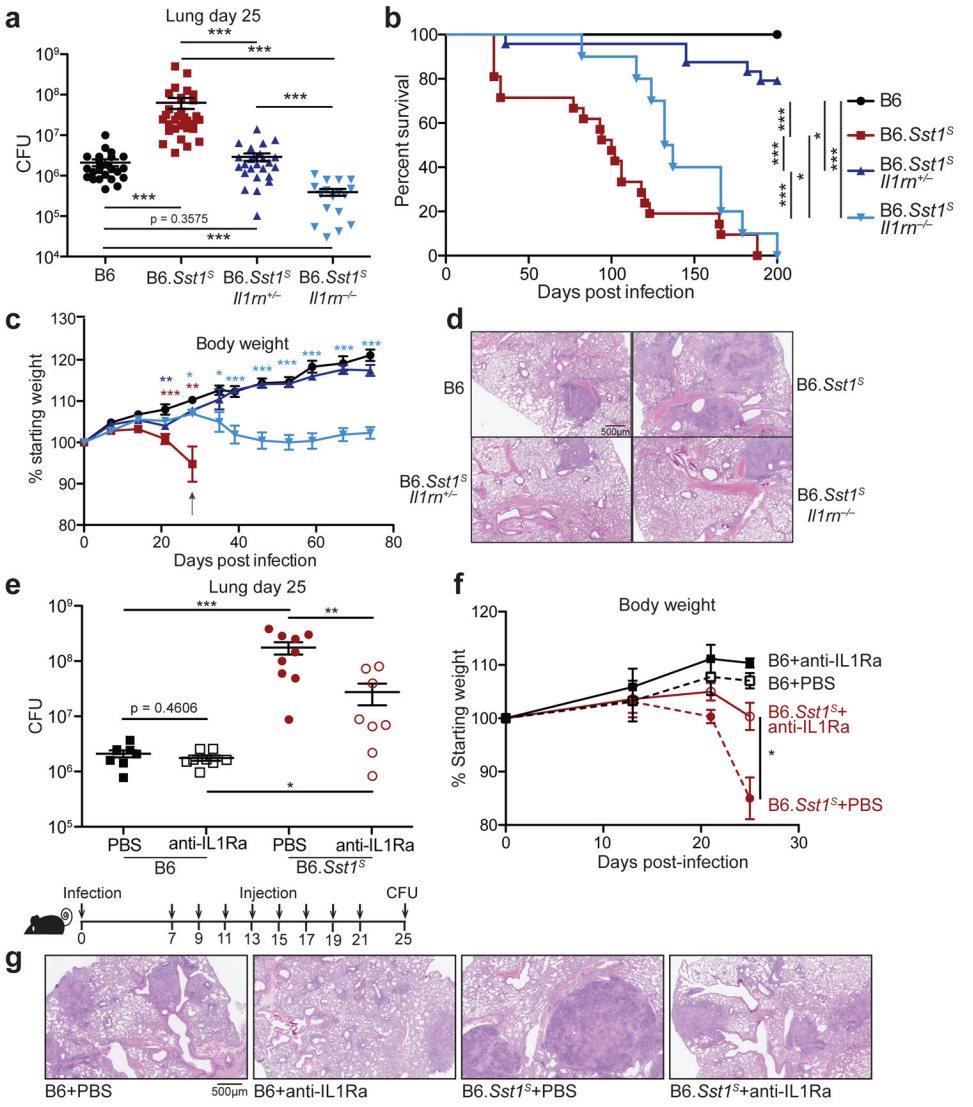

Fig. 4 |. Inhibition of IL-1Ra rescues the susceptibility of B6.*Sst1*^{S} mice.

a-d, *Mtb*-infected mice (20CFU/mouse) were measured for (**a**) bacterial burdens in the lungs at day 25, (**b**) survival, (**c**) body weight or (**d**) lung sections were stained with hematoxylin and eosin (H&E) for histology. For **c**, arrow indicates where 4/21 mice reached end-point. Color of statistics indicates relevant genotype as compared to B6. **e-g**, *Mtb*-infected mice (32CFU/mouse) were treated with anti-IL1Ra antibody or PBS and (**d**) lung bacterial burdens were measured at day 25, or (**f**) day 25 lung sections were stained with H&E, or (**e**) body weights were recorded over time. Combined results of four (**a**) or two (**b**) experiments. **c**, **d-g**, representative results of two experiments. Sample size n (**a-c**): B6, B6.*Sst1*^{S}, B6.*Sst1*^{S}*Il1rn*$^{+/-}$, B6.*Sst1*^{S}*Il1rn*$^{-/-}$ = 24, 30, 25, 17 (**a**); 17, 21, 24, 10 (**b**); 11, 12, 21, 10 (**c**). Sample size n (**e-f**): B6 PBS =8, B6 anti-IL1Ra = 8, B6.*Sst1*^{S} PBS = 9, B6.*Sst1*^{S} anti-IL1Ra = 8. All were bred in-house, and all except B6 and B6.*Sst1*^{S} were littermates (**a-d**); B6.*Sst1*^{S} were bred in-house (**e-g**). Center and error bars show mean and SEM. Analyzed with two-

ended Mann-Whitney test (**a**, **c**, **e**, **f**) or two-ended Log-rank test (**b**). Asterisk, $p \leq 0.05$; two asterisks, $p \leq 0.01$; three asterisks, $p \leq 0.001$.